Usefulness of Macular Thickness Derived from Spectral-Domain Optical Coherence Tomography in the Detection of Glaucoma Progression

Kyoung Sub Lee,[1] *Jong Rak Lee,*[1] *Jung Hwa Na,*[1,2] *and Michael S. Kook*[1]

Purpose. To assess the reproducibility of circumpapillary retinal nerve fiber layer thickness (cRNFLT) and total macular thickness (TMT) parameters using Cirrus spectral domain optical coherence tomography (SD-OCT) and to apply this information to investigate its ability to detect cases where visual field (VF) progression was noted on event-based analysis in the eyes with early glaucomatous VF loss.

Methods. Intraclass correlation coefficient (ICC), coefficient of variation (COV), and intersession test–retest variability were calculated from the control group. The sensitivity and specificity of SD-OCT for the identification of progressive VF defects were tested on progressive and stable patients.

Results. All ICCs from cRNFLT and TMT measurements ranged from 94.8% to 99.0%. While average cRNFLT showed the lowest intersession COV (2.57%), the nasal-outer and superior-inner TMT sectors showed the lowest COV (0.96%). The sensitivities of Cirrus SD-OCT cRNFLT measurements ranged from 37.8% to 48.9%, while that of TMT measurement was 73.3% when tested at the 95% confidence interval (CI). The sensitivity for detecting progressive VF changes in the central 10° area improved to 84.8% with TMT measurement, while it remained unchanged with cRNFLT measurements. The agreement on progression detection between cRNFLT and TMT sector measurements was poor ($\kappa = 0.072$ for overall, and 0.102 for the central 10° area at 95% CI, respectively).

Conclusions. Intersession measurements of both cRNFLT and TMT parameters with Cirrus SD-OCT showed excellent reproducibility. TMT parameters using Cirrus SD-OCT may be better than cRNFLT measurements in terms of detecting progressive VF loss. This sensitivity derived from TMT measurements increased when progressive VF loss occurred in the central 10° area. (*Invest Ophthalmol Vis Sci.* 2013; 54:1941–1949) DOI:10.1167/iovs.12-11160

From the [1]Department of Ophthalmology, University of Ulsan, College of Medicine, Asan Medical Center, Seoul, Korea; and the [2]Department of Ophthalmology, Konyang University, Kim's Eye Hospital, Myung-Gok Eye Research Institute, Seoul, Korea.

Presented in part as a poster at the annual meeting of the Association for Research in Vision and Ophthalmology, Fort Lauderdale, Florida, May 2012.

The authors alone are responsible for the content and writing of the paper.

Submitted for publication October 17, 2012; revised January 10 and February 7, 2013; accepted February 8, 2013.

Disclosure: **K.S. Lee**, None; **J.R. Lee**, None; **J.H. Na**, None; **M.S. Kook**, None

Corresponding author: Michael S. Kook, Department of Ophthalmology, University of Ulsan, College of Medicine, Asan Medical Center, 388-1 Pungnap-2-dong, Songpa-gu, Seoul, Korea 138-736; mskook@amc.seoul.kr.

Glaucoma is an optic neuropathy that results in both progressive structural change and/or functional visual field (VF) loss.[1] To date, progression detection remains one of the most difficult challenges of glaucoma management. Although current methods for detecting glaucoma progression in clinical trials and population-based studies rely on visual field testing, a variety of methods to detect progression have been introduced ranging from a subjective clinical judgment based on observers to complex statistical analyses of many observations over time acquired from both glaucoma imaging devices as well as visual field testing (trend-based analysis). Therefore, study outcomes in terms of detecting progression are highly dependent on the method of defining progression used, and currently there is no gold standard by which the performance of various methods can be compared.

In everyday practice, event-based VF analysis is more often utilized than trend-based analysis in the form of either a subjective manner or by means of a commercially available perimetry software (STATPAC; Carl Zeiss Meditec Inc., Dublin, CA) program in which follow-up examination is compared with a baseline of a single examination or a mean of two or more examinations. With VF testing, the changes are compared to the test–retest variability from a separate sample of patients. If the observed VF changes exceed the test–retest limits, which are typically estimated by the empirical fifth and 95th percentile, in a given number of test locations on a given number of consecutive follow-up examinations, we consider that actual change is likely to have occurred. Similar to VF testing, glaucoma progression using structural imaging devices such as spectral-domain optical coherence tomography (SD-OCT) can be defined on the basis of a somewhat arbitrarily chosen cut-off; for instance, can be defined on the basis of the thickness changes that exceed the test–retest variability from a separate sample of patients, as estimated by empirical fifth and 95th percentiles on 2 or more consecutive follow-up examinations. Although the event-based analysis using VF testing is frequently used in the detection of glaucoma progression, it remains unclear, or there is a limited knowledge, whether a similar approach utilizing SD-OCT can be feasible to detect glaucoma progression in a clinical setting.

Measurement of macular thickness is important in diagnosis and monitoring of glaucomatous change.[2–4] The use of experimental primate models of glaucoma has shown that ganglion cells in the fovea region seem to be vulnerable to glaucomatous injury, and that ganglion cell loss occurs even if glaucomatous changes were mild.[5] In humans, loss of ganglion cells and reduced nerve fiber thickness has also been observed in the posterior pole region of glaucomatous eyes even at early stages of the disease.[6] The clinical utility of measuring both circumpapillary retinal nerve fiber layer thickness (cRNFLT) and macular thickness in terms of glaucoma detection has been proven in numerous studies.[7–15] However, there is limited knowledge as to whether macular thickness measurement has

the capability to detect progressive change in early glaucomatous eyes.

Although numerous studies have reported good reproducibility of cRNFLT measurement derived from SD-OCT,[16–20] the reproducibility of macular thickness derived from SD-OCT and its application to glaucoma progression detection has not been fully elucidated. With this in mind, in the current study, we used the SD-OCT equipment (Cirrus HD; Carl Zeiss Meditec Inc.) to investigate intersession reproducibility characterized by intraclass correlation (ICC), coefficients of variation (COVs), and intersession test–retest variability of total macular thickness (TMT) as well as cRNFLT in stable eyes with early glaucomatous VF loss (control group). In addition, we evaluated whether TMT assessment could be used to detect cases where VF progression was noted on event-based analysis in the eyes with early glaucomatous VF loss and compared its ability with that of cRNFLT measurement. Finally, eyes with normal-tension glaucoma (NTG) often exhibit scotomas and progress close to the fixation point.[7,21] Thus, to test the progression detection capabilities of cRNFLT and TMT data with respect to VF defect location, we performed a secondary analysis in the eyes with VF progression involving the central 10 degrees.

Methods

Patients

One hundred seventy-six glaucoma patients with early glaucomatous VF loss (baseline mean deviation [MD] better than −10 dB) who were evaluated between January 2008 and October 2012 at the glaucoma clinic of the Asan Medical Center, Seoul, Korea, and met our inclusion criteria, were included by retrospective medical record review.

At initial testing, each participant received a comprehensive ophthalmologic examination, including a review of medical history; measurement of best-corrected visual acuity (BCVA); slit-lamp biomicroscopy; Goldmann applanation tonometry (GAT); gonioscopy; dilated funduscopic examination using a 90 (diopter [D]) lens; stereoscopic optic disc photography; retinal nerve fiber layer (RNFL) photography; second VF test to obviate any learning effect when first VF showed glaucomatous VF change (using a Humphrey Field Analyzer [HFA] running the Swedish Interactive Threshold Algorithm [SITA] 24-2; Carl Zeiss Meditec Inc.), and SD-OCT (Cirrus HD-OCT; Carl Zeiss Meditec Inc.).

For inclusion in the study, all participants had to have open angle glaucoma (OAG) regardless of IOP level with the following criteria: BCVA of 20/30 or better, with a spherical equivalent within ±5 D and a cylinder correction within +3 D; presence of a normal anterior chamber and open angle on slit-lamp and gonioscopic examinations; two reliable HFA test results with a false-positive error $< 15\%$, a false-negative error $< 15\%$, and a fixation loss $< 20\%$.

Glaucomatous eyes in our study were defined as having glaucomatous VF defects confirmed by at least two reliable VF examinations and the presence of a compatible glaucomatous optic disc that showed increased cupping (a vertical and/or horizontal cup-disc [C/D] ratio $>$ 0.6); a difference in vertical C/D ratio of $>$0.2 between eyes that was unrelated to differences in disc size; diffuse or focal neural rim thinning; and disc hemorrhage or RNFL defects. Eyes with glaucomatous VF defects were defined as those with a cluster of three points with probabilities of 5% on the pattern deviation (PD) map in at least one hemifield, including at least one point with a probability of 1% or a cluster of two points with a probability of 1%, and a glaucoma hemifield test (GHT) result outside normal limits or a pattern standard deviation (PSD) outside 95% of the normal limits. One eye was randomly selected if both eyes were found to be eligible for inclusion in the study. Patients with any other ophthalmic or neurologic condition that could result in a VF defect were excluded. If surgical or laser treatment was performed during follow-up, only the data obtained in the period before such treatment were analyzed.

Among patients who qualified using the initial criteria, each eye for which the second VF testing mean deviation (MD) value was better than −10 dB was included in the final analysis, as this study attempted to evaluate the capability of SD-OCT (Carl Zeiss Meditec Inc.) TMT and cRNFLT measurements to detect progression in glaucoma patients with early VF loss. All glaucomatous patients were followed up at 6-month intervals via VF testing, stereoscopic optic disc photography, RNFL photography, and SD-OCT (Carl Zeiss Meditec Inc.) scanning, with a minimum follow-up of 4 years. All tests were performed at the same visit or within 2 weeks of that visit. The mean number of VF testing and SD-OCT (Carl Zeiss Meditec Inc.) scanning were 8.2 ± 1.2, 8.1 ± 0.8, respectively. For the purpose of the present study, three patient groups meeting defined eligibility criteria were used based on VF testing: first, a progressive glaucoma group to test SD-OCT (Carl Zeiss Meditec Inc.) sensitivity; second, a stable glaucoma group to test SD-OCT specificity; and third, a control group who were stable glaucoma patients to establish test–retest limits. Institutional review board approval was obtained from the Asan Medical Center and our study design followed the principles of the Declaration of Helsinki.

Patients with Stable Glaucoma

Eligible patients with stable glaucoma were consecutively enrolled in the study during regular follow-up visits and were divided into two groups: control group 1 ($n = 42$), whose data were used to measure SD-OCT (Carl Zeiss Meditec Inc.) reproducibility and stable group 2 ($n = 40$), whose data were used to evaluate SD-OCT (Carl Zeiss Meditec Inc.) specificity in the detection of progressive VF change. For control group 1, we also performed a subgroup analysis of reproducibility according to disease severity. Stable glaucoma was defined as no significant deterioration of single point from the baseline pattern deviation (PD) throughout follow-up VFs.

Patients with Progressive Glaucomatous Change

Eyes ($n = 45$) showing progressive glaucomatous VF changes that met eligibility criteria were enrolled consecutively. Progressive visual field change was determined by event-based analysis using commercial software (HFA; Carl Zeiss Meditec Inc.).

Determination of Glaucoma Stability or Progression by VF

All patients had undergone at least three or more reliable visual field tests in addition to an initial established baseline VF after excluding the first VF to obviate the learning effect. VF progression was defined as a significant deterioration from the baseline PD at three or more of the same test points evaluated on three consecutive examinations. When this criteria was not fully met (e.g., in those eyes with only two progressing points on two or three consecutive tests), these eyes were excluded from the study.

Optical Coherence Tomography

SD-OCT images were obtained using the HD-OCT system (Carl Zeiss Meditec Inc.). Our HD-OCT (Carl Zeiss Meditec Inc.) platform is calibrated on a regular basis by a technician employed by the manufacturer. The same OCT (Carl Zeiss Meditec Inc.) instrument was used by the same operator for all testing sessions. Pupil dilation was performed as needed. All accepted images exhibited a centered optic disc; were well-focused, with even and adequate illumination; exhibited no eye motion within the measurement circle; and had signal strength (SS) greater than or equal to 7. For inclusion in the progression analysis, at least five acceptable OCT images, obtained at separate visits, were required in both stable and progressive groups

and all images had to meet the requirements for image quality to be included in the analysis.

Optic disc cube data were obtained from a 3-dimensional dataset composed of 200 A-scans derived from 200 B-scans that covered a 6×6 mm area centered on the optic disc. After creation of an RNFL thickness map from the cube dataset, the software equipped in the Cirrus HD-OCT (Carl Zeiss Meditec Inc.) automatically determines the center of the disc and then extracts a circumpapillary circle (1.73 mm in radius) from the dataset to perform RNFL thickness measurements. The RNFL thicknesses of the four quadrants (temporal, superior, nasal, and inferior) and average RNFL thickness were used as cRNFLT parameters.

The macula was scanned using the macular cube mode and the data were obtained from a 3-dimensional dataset composed of 512 A-scans derived from 128 B-scans that cover a 6 mm^2 area centered on the fovea. The macular thicknesses of nine sectors (temporal outer, superior outer, nasal outer, inferior outer, temporal inner, superior inner, nasal inner, inferior inner, and fovea) were used as TMT parameters in the analysis.

Topographic Match of VF to cRNFLT and TMT Sector

The map of Ferreras et al. was used to determine clock-hour RNFL sectors corresponding to worsening VF points on HFA GPA.[22] In brief, each hemifield was divided into five VF regions matched with SD-OCT cRNFLT clock-hours upon factor analysis. In a given region of worsening VF points, an overlap in the quadrant representation of cRNFLT abnormalities can occur, in which all overlapping quadrants were analyzed for topographic match. Currently, there is no established structure-function match between VF and early treatment diabetic retinopathy study (ETDRS) subfields map. In macula, fibers from the temporal periphery originate on either side of a horizontal dividing line, the median raphe, and travel above or below the fovea as the arcuate fibers, while those from the central retina, the papillomacular fibers, and the nasal fibers travel directly to the nerve head. Therefore, superior progressive VF points were matched to inferior, nasal, and temporal inner and outer sectors while inferior progressive VF points were matched to superior, nasal, and temporal inner and outer sectors in the TMT map.

Data Analysis

One-way ANOVA test was used for comparisons among three groups. For control group 1 ($n = 42$), we obtained data on ICC (2,1); COVs; and intersession test–retest variability for the 360° average, quadrant cRNFLT, and nine-sector TMT from the first and second data. These eyes were further divided into two groups (< -3 dB, $n = 21$ vs. ≥ -3 dB, $n = 21$) based on the median MD value of control group 1 to compare reproducibility. For the purpose of the present study, intersession test–retest variability was defined at the 95% and 80% confidence level. It was calculated as 1.96-fold greater than the intervisit standard deviation (SD) for the 95% level and was calculated as 1.28-fold greater than the intervisit SD for the 80% level. The number of patients and measurements were sufficient to establish the lower 95% confidence limit for an ICC of 0.85 as not being lower than 0.75.

The sensitivity and specificity of HD SD-OCT (Carl Zeiss Meditec Inc.) were tested using the following: cRNFLT decreased beyond the limit in 360° average thickness; cRNFLT decreased beyond the limit in one or more than one quadrant (≥1 quadrant in cRNFLT); and TMT decreased beyond the limit in one or more than one sector (≥1 sector in TMT) on two consecutive exams in all three criteria. The specificity of SD-OCT in the stable group was tested with SD-OCT (Carl Zeiss Meditec Inc.) data from the latest visit. Comparison of sensitivity and specificity for the detection of VF progression between two anatomical sites were performed using the McNemar's test.

To test the progression detection capabilities of cRNFLT and TMT data with respect to VF defect location, the 24-2 field was divided into two areas: within the central 10° region, and within the 10° to 24° area (Fig. 1). For central VF progression, we used the modified Anderson criteria (MAC).[23] Briefly, central 10° VF progression was defined as a significant deterioration from the baseline PD if three or more points in the central 10° have deteriorated by 10 dB at the same test points evaluated on three consecutive examinations. If the eyes with a single cluster of three adjacent points overlap at both the central 10° and the peripheral 10° to 24° region, based on the PD plot, 2 points must be located in the central 10°.

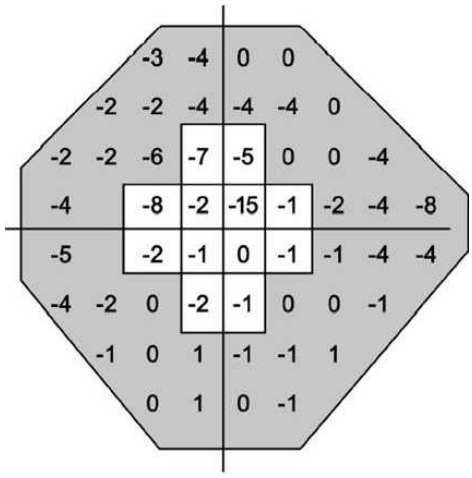

Figure 1. The central 10° region of the Humphrey 24-2 visual field was determined as illustrated. Two test locations within the blind spot and 10° to 24° (*shaded area*) were excluded.

The agreement between cRNFLT and TMT measurements in detecting VF progression was calculated with the kappa (κ) test.[24] Finally, the frequency of topographic match between the corresponding SD-OCT parameters and worsening VF points in progressive group was analyzed. Statistical analyses were performed with commercial software (SPSS 18.0; SPSS Inc., Chicago, IL). $P < 0.05$ was considered to indicate a significant difference.

Results

The study initially included 176 glaucomatous eyes of 176 patients. The 49 eyes were excluded due to poor quality of OCT images, such as low signal strength (17 eyes, SS < 7); motion artifact (10 eyes); decentration (eight eyes); or unacceptable VF test (14 eyes). Finally, a total of 127 glaucomatous eyes from 127 patients were included. The mean follow-up period was 4.6 ± 0.52 years. Table 1 shows the demographic and baseline characteristics of three groups. There were no statistical significances among the three groups in terms of age at the time of enrollment, initial cRNFLT, MD, and pattern standard deviation (PSD; $P > 0.05$).

Reproducibility of SD-OCT cRNFLT and TMT

Table 2 shows the intersession variability data from the control group obtained on the first two separate visits. Intersession ICCs were excellent for all cRNFLT parameters, with the nasal quadrant showing the lowest values (0.948) and the superior quadrant cRNFLT with the highest values (0.989). ICCs were also excellent for all TMT parameters and ranged between 0.96 and 0.99. COVs were all under 10%. Among the cRNFLT parameters, average cRNFLT showed the lowest intersession COV (2.57%). Among the TMT parameters, the nasal-outer and superior-inner sectors showed the lowest COV (0.96%). The test–retest variability defined at the 95% level for average

Table 1. Patient Demographics

	Progression Group, $N = 45$	Stable Group, $N = 40$	Control Group, $N = 42$	P^*
Age, y, mean ± SD	56.0 ± 14.1	56.3 ± 16.1	53.1 ± 15.9	0.476
Initial average cRNFLT, μm, mean ± SD	73.44 ± 12.32	75.48 ± 10.34	75.47 ± 12.52	0.662
MD, dB, mean ± SD (range)	−4.59 ± 2.82 (−1.50 ~ −8.00)	−3.00 ± 2.53 (−1.50 ~ −6.00)	−4.80 ± 5.89 (−1.50 ~ −8.00)	0.181
PSD, dB, mean ± SD	4.64 ± 3.02	4.04 ± 2.84	5.07 ± 4.16	0.398

* One-way ANOVA test.

cRNFLT was 3.78 μm while it was 5.29 μm for the nasal outer TMT sector. Subgroup analysis according to disease severity showed similar reproducibility data between the two groups (Table 3).

Sensitivity and Specificity of SD-OCT cRNFLT and TMT Parameters for the Detection of Progressive Glaucoma according to HFA GPA Criteria

Table 4 shows the sensitivities of SD-OCT (Carl Zeiss Meditec Inc.), which were tested using criteria that corresponded to the upper 95% limit of test–retest variability defined at the 95% and 80% levels. At the 95% level, the sensitivity was higher for the criterion based on TMT (in ≥1 sector in TMT) compared with cRNFLT (in ≥1 quadrant in cRNFLT). This difference is statistically significant ($P = 0.027$). At the 80% level, our results showed a similar trend with statistical significance ($P = 0.013$). The specificity was similar for both criteria based on cRNFLT parameters compared with TMT parameters without statistically significant difference (Table 5).

Sensitivity of SD-OCT cRNFLT and TMT Parameters for the Detection of Progressive Glaucoma Identified in the Central 10° Area according to MAC

We consecutively selected eyes with VF progression involving the central 10° area from the total of 45 progressive eyes. Among 45 eyes, 33 eyes (73%) progressed in the central 10° VF area. As expected, at both the 95% and 80% level, the sensitivity of detecting VF progression in the central 10° area was higher for TMT parameters (in ≥1 sector in TMT) compared with cRNFLT parameters (in ≥1 quadrant in cRNFLT). This difference was statistically significant ($P < 0.001$, 0.021, respectively, Table 6).

Agreement between cRNFLT (Quadrant, Average) and TMT (≥1 Sector in TMT) Parameters to Detect VF Progression

The agreement for progression detection between two anatomical sites was poor, with κ values of 0.072 and 0.122 for quadrant and average data, respectively, at the 95% level and 0.079 and 0.136 for quadrant and average data, respectively, at the 80% level. The agreement for progression at the central 10° VF area was also poor, with κ values of 0.102 and 0.083 for quadrant and average data, respectively, at the 95% level, and 0.166 and 0.137 for quadrant and average data, respectively, at the 80% level (Figs. 2, 3).

Frequency of Topographic Match between TMT Parameters and cRNFLT and VF Progression Points in Progressive Group

Thirty eyes (90.9%) of 33 progressive eyes based on TMT criteria (in ≥1 sector in TMT) at the 95% level showed a topographic match while 19 eyes (86.4%) of 22 progressive eyes based on cRNFLT criteria (in ≥1 quadrant in cRNFLT) at the 95% level showed a topographic match with GPA progression location. In the eyes with central 10° VF progression, 26 eyes (92.8%) of 28 progressive eyes based on TMT criteria (in ≥1 sector in TMT) at the 95% level revealed a topographic match, while 11 eyes (84.6%) of 13 progressive eyes based on cRNFLT criteria (in ≥1 quadrant in cRNFLT) at the 95% level revealed a topographic match with GPA progression location. Similar frequency of topographic match

Table 2. Intraclass Correlation and Intersession Test–Retest Variability of SD-OCT Measurements ($N = 42$)

Location	ICC (95% CI)*	COV, %	Test–Retest Variability 95%, μm† (SD × 1.96)	Test–Retest Variability 80%, μm‡ (SD × 1.28)
Average cRNFL	0.987 (0.975–0.993)	2.57	3.78 (2.82–4.67)	2.48 (1.84–3.05)
Temporal cRNFL	0.985 (0.972–0.992)	4.48	5.43 (3.34–7.08)	3.54 (2.18–4.62)
Superior cRNFL	0.989 (0.980–0.994)	3.01	5.27 (3.81–6.64)	3.44 (2.49–4.34)
Nasal cRNFL	0.948 (0.904–0.972)	3.13	6.14 (4.53–7.52)	4.01 (2.96–4.91)
Inferior cRNFL	0.986 (0.974–0.992)	4.17	7.11 (4.89–9.02)	4.64 (3.19–5.89)
Temporal-outer macular	0.960 (0.926–0.979)	1.86	8.91 (4.22–12.95)	5.82 (2.76–8.46)
Superior-outer macular	0.974 (0.951–0.986)	1.47	7.54 (4.35–10.17)	4.92 (2.84–6.64)
Nasal-outer macular	0.990 (0.981–0.995)	0.96	5.29 (4.05–6.52)	3.46 (2.65–4.26)
Inferior-outer macular	0.981 (0.965–0.990)	1.57	7.59 (5.08–9.60)	4.96 (3.32–6.27)
Temporal-inner macular	0.984 (0.969–0.991)	1.09	6.29 (4.22–7.97)	4.11 (2.76–5.21)
Superior-inner macular	0.987 (0.976–0.993)	0.96	5.79 (3.84–7.40)	3.78 (2.51–4.83)
Nasal-inner macular	0.985 (0.973–0.992)	0.97	5.99 (3.65–7.97)	3.91 (2.38–5.20)
Inferior-inner macular	0.986 (0.974–0.993)	1.09	6.42 (4.45–8.19)	4.19 (2.90–5.35)
Central macular	0.989 (0.980–0.994)	1.43	7.01 (4.99–8.57)	4.58 (3.26–5.60)

* Shown with lower 95% CI in parentheses.
† Test–retest variability is defined at the 95% level shown with 95% CI in parentheses.
‡ Test–retest variability is defined at the 80% level shown with 95% CI in parentheses.

Table 3. Intraclass Correlation and Intersession Test–Retest Variability of SD-OCT Measurements ($N = 21$, <-3 dB versus $N = 21$, ≥ -3 dB)

Location	ICC (95% CI)*		COV, %		Test–Retest Variability 95%, μm†, (SD × 1.96)		Test–Retest Variability 80%, μm‡, (SD × 1.28)		P§
	<-3 dB	≥ -3 dB	<-3 dB	≥ -3 dB	<-3 dB	≥ -3 dB	<-3 dB	≥ -3 dB	
Average cRNFL	0.987 (0.975–0.993)	0.985 (0.964–0.994)	2.57	2.55	3.78 (2.82–4.67)	3.33 (2.31–4.08)	2.48 (1.84–3.05)	2.17 (1.51–2.66)	0.387
Temporal cRNFL	0.985 (0.972–0.992)	0.973 (0.935–0.989)	4.48	4.39	5.43 (3.34–7.08)	4.53 (1.92–6.86)	3.54 (2.18–4.62)	2.96 (1.25–4.48)	0.622
Superior cRNFL	0.989 (0.980–0.994)	0.991 (0.977–0.996)	3.01	2.52	5.27 (3.81–6.64)	3.89 (2.27–4.82)	3.44 (2.49–4.34)	2.54 (1.48–3.15)	0.256
Nasal cRNFL	0.948 (0.904–0.972)	0.952 (0.882–0.981)	3.13	5.09	6.14 (4.53–7.52)	6.01 (3.91–7.34)	4.01 (2.96–4.91)	3.93 (2.55–4.79)	0.847
Inferior cRNFL	0.986 (0.974–0.992)	0.981 (0.953–0.992)	4.17	5.36	7.11 (4.89–9.02)	7.85 (4.15–10.67)	4.64 (3.19–5.89)	5.12 (2.71–6.96)	0.867
Temporal-outer macular	0.960 (0.926–0.979)	0.890 (0.729–0.955)	1.86	2.48	8.91 (4.22–12.95)	11.55 (4.90–16.71)	5.82 (2.76–8.46)	7.54 (3.20–10.91)	0.479
Superior-outer macular	0.974 (0.951–0.986)	0.957 (0.895–0.983)	1.47	1.85	7.54 (4.35–10.17)	9.23 (3.71–12.55)	4.92 (2.84–6.64)	6.03 (2.42–8.20)	0.586
Nasal-outer macular	0.990 (0.981–0.995)	0.993 (0.984–0.997)	0.96	0.85	5.29 (4.05–6.52)	4.56 (3.47–5.26)	3.46 (2.65–4.26)	2.98 (2.27–3.44)	0.537
Inferior-outer macular	0.981 (0.965–0.990)	0.946 (0.867–0.978)	1.57	1.94	7.59 (5.08–9.60)	9.01 (5.20–11.93)	4.96 (3.32–6.27)	5.88 (3.40–7.79)	0.366
Temporal-inner macular	0.984 (0.969–0.991)	0.970 (0.926–0.988)	1.09	1.13	6.29 (4.22–7.97)	6.31 (4.35–7.76)	4.11 (2.76–5.21)	4.12 (2.84–5.07)	0.215
Superior-inner macular	0.987 (0.976–0.993)	0.995 (0.986–0.998)	0.96	0.60	5.79 (3.84–7.40)	3.56 (2.59–4.24)	3.78 (2.51–4.83)	2.33 (1.69–2.77)	0.106
Nasal-inner macular	0.985 (0.973–0.992)	0.993 (0.983–0.997)	0.97	0.64	5.99 (3.65–7.97)	3.89 (2.08–5.25)	3.91 (2.38–5.20)	2.54 (1.35–3.43)	0.585
Inferior-inner macular	0.986 (0.974–0.993)	0.984 (0.961–0.994)	1.09	0.97	6.42 (4.45–8.19)	5.49 (3.48–6.93)	4.19 (2.90–5.35)	3.58 (2.27–4.52)	0.516
Central macular	0.989 (0.980–0.994)	0.988 (0.970–0.995)	1.43	1.65	7.01 (4.99–8.57)	8.05 (4.27–10.47)	4.58 (3.26–5.60)	5.26 (2.79–6.83)	0.933

* Shown with lower 95% CI in parentheses.
† Test–retest variability is defined at the 95% level shown with 95% CI in parentheses.
‡ Test–retest variability is defined at the 80% level shown with 95% CI in parentheses.
§ Comparison of test–retest variability at the 95% level between <-3 dB and ≥ -3 dB groups (independent *t*-test).

Table 4. Sensitivity of SD-OCT cRNFLT and TMT Parameters for Detection of Progressive Glaucoma Based on HFA GPA Criteria ($N = 45$)

In ≥1 Quadrant in cRNFL (%)	In ≥1 Macular Area Thickness (%)	P*
Sensitivity†		
48.9 (40.0–71.1)	73.3 (51.1–91.1)	0.027
48.9 (40.0–71.1)	37.8 (33.3–44.4)‡	0.063
37.8 (33.3–44.4)‡	73.3 (51.1–91.1)	0.001
Sensitivity§		
62.2 (55.6–77.8)	86.7 (86.7–95.6)	0.013
62.2 (55.6–77.8)	44.4 (40.0–55.6)‡	0.008
44.4 (40.0–55.6)‡	86.7 (86.7–95.6)	<0.001

* McNemar's test.
† Upper 95% limit of test–retest variability defined at the 95% confidence level.
‡ Average cRNFLT.
§ Upper 95% limit of test–retest variability defined at the 80% confidence level.

was also noted in both criteria at the 80% level (data not shown).

Discussion

In the current study, we used the HD SD-OCT (Carl Zeiss Meditec Inc.) to investigate the reproducibility of TMT and cRNFLT measurements in stable eyes with early glaucomatous VF loss. Subsequently, we used this information to evaluate the sensitivity and specificity of TMT and cRNFLT measurements in glaucomatous eyes with confirmed VF progression and stable glaucomatous eyes using event-based analysis. We found that average cRNFLT showed the lowest intersession COV (2.57%) while the nasal-outer and superior-inner TMT sectors showed the lowest COV (0.96%). The sensitivities of cRNFLT measurements ranged from 37.8% to 48.9%, while that of TMT measurement was 73.3% when tested at the 95% confidence level.

The reproducibility of the cRNFLT measurements in the current study was very similar to those reported recently by Mwanza et al.[16] In both studies, it was found that there was less test–retest variability for average cRNFLT than for quadrant thickness. This result is also in agreement with other studies, despite the fact that COV was based on intravisit reproducibility of cRNFLT measured using other SD-OCT devic-

Table 5. Specificity of SD-OCT RNFLT and TMT Parameters for Detection of Progressive Glaucoma Based on HFA GPA Criteria ($N = 40$)

	In ≥1 Quadrant in cRNFL (%)	In ≥1 Macular Area Thickness (%)	P*
Specificity†			
	75.0 (60.0–82.5)	77.5 (62.5–90.0)	1.000
	75.0 (60.0–82.5)	85.0 (82.5–90.0)‡	0.344
	85.0 (82.5–90.0)‡	77.5 (62.5–90.0)	0.453
Specificity§			
	57.5 (45.0–62.5)	62.5 (40.0–72.5)	0.687
	57.5 (45.0–62.5)	82.5 (77.5–85.0)‡	0.022
	82.5 (77.5–85.0)‡	62.5 (40.0–72.5)	0.065

* McNemar's test.
† Upper 95% limit of test–retest variability defined at the 95% confidence level.
‡ Average cRNFLT.
§ Upper 95% limit of test–retest variability defined at the 80% confidence level.

Table 6. Sensitivity of SD-OCT cRNFLT and TMT Parameters for the Detection of Progressive Glaucoma Based on Modified Anderson Criteria at Central 10° Region ($N = 33$)

	In ≥1 Quadrant in cRNFL (%)	In ≥1 Macular Area Thickness (%)	P*
Sensitivity†	39.4 (33.3–57.6)	84.8 (51.5–90.9)	<0.001
	39.4 (33.3–57.6)	36.4 (30.0–42.4)‡	1.000
	36.4 (30.0–42.4)‡	84.8 (51.5–90.9)	<0.001
Sensitivity§			
	66.6 (60.6–72.7)	90.9 (90.9)	0.021
	66.6 (60.6–72.7)	42.4 (39.4–51.5)‡	0.008
	42.4 (39.4–51.5)‡	90.9 (90.9)	<0.001

* McNemar's test.

† Upper 95% limit of test–retest variability defined at the 95% confidence level.

‡ Average cRNFLT.

§ Upper 95% limit of test–retest variability defined at the 80% confidence level.

es.[20,25–27] Similar findings have also been noted in studies using both TD- and SD-OCT devices.[9,18,28]

The present study found excellent intersession reproducibility of TMT measurements based on the ICCs, COVs, and test–retest variability. Garas et al.[28] evaluated the reproducibility of GCC thickness in the macula and found that intersession COVs were <3%. Although different thicknesses in the macula using different SD-OCT devices were measured in the current study, our results were similar to that reported in stable glaucomatous eyes with COVs being less than 2%. In concordance with the results by Garas et al., the reproducibility derived from TMT as indicated by COV was better than that of the cRNFLT measurement.

Increased test–retest variability with a different spectrum of disease severity has been found with VF testing, in which threshold variability increases with advancing glaucoma.[29–33] Therefore, the HFA GPA reflects this phenomenon in its reference database across different stages of visual function. Prior studies evaluating the reproducibility of various imaging devices assumed that the reproducibility of measures with different devices would be the same across all stages of visual function.[34–37] Recently, DeLeon Ortega et al. reported that test–retest variability of cRNFLT using different devices (GDx-VCC and StratusOCT; Carl Zeiss Meditec Inc.) were consistent at early stages of glaucoma except in severe cases.[38] Of interest, we also found no significant differences in test–retest variability of TMT and cRNFLT parameters between two subgroups within the eyes at early stages of glaucoma.

Currently, there is a paucity of published studies reporting the clinical utility of both cRNFLT and posterior pole macular thickness measurements to detect glaucoma progression.[25,39] In these cited studies, the sensitivities of various macular thicknesses as well as cRNFLT measurements in glaucoma progression detection were not good (5%–14%) despite high specificities, which was in line with previous studies using other structural imaging devices.[40–46] The explanations for low sensitivities were attributable to relatively short follow-up times (mean = 2.13 years) and a low number of OCT examinations (cRNFL: mean = 4.5 and macula: mean = 4.6) during follow-up.

In the current study, TMT sector criterion appeared to be more sensitive than either the average or quadrant cRNFLT criteria, particularly at the 95% upper limit of test–retest variability defined at the 95% confidence level ($P = 0.001$, 0.027, respectively, Table 4). A similar trend was also noted at the 95% upper limit of test–retest variability defined at the 80% confidence level ($P < 0.001$, 0.013, respectively, Table 4). These findings are somewhat expected from the measurements

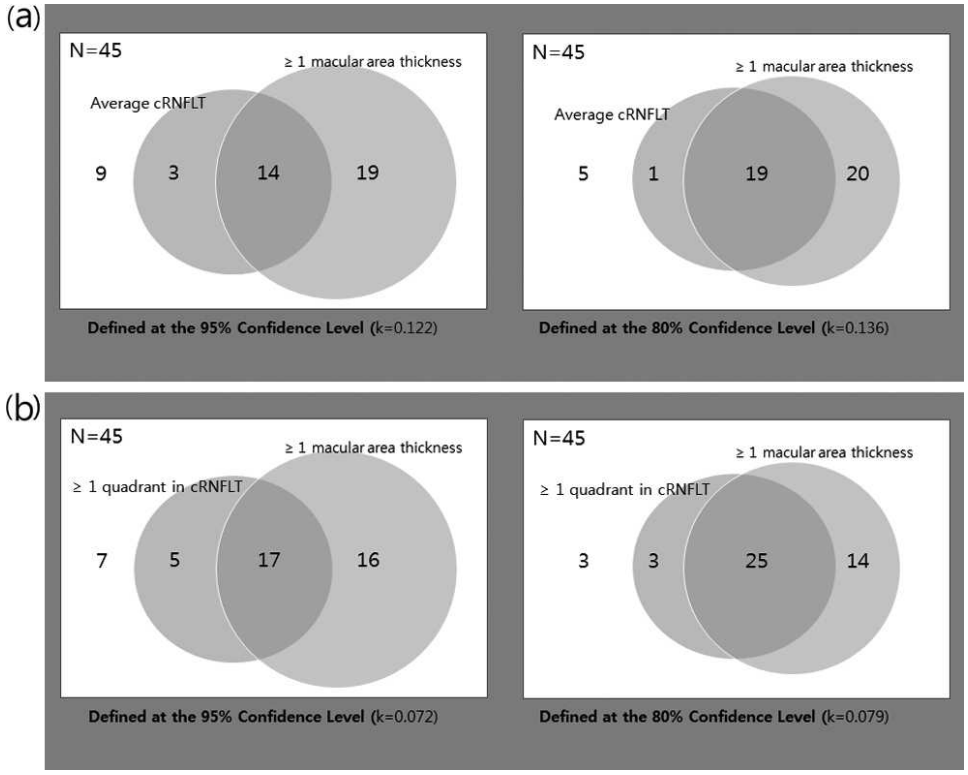

Figure 2. An area-proportional Venn diagram showing agreement in terms of overall glaucoma progression detection when average cRNFLT and ≥1 sector in TMT were used to this end in (**a**) and when ≥1 quadrant in cRNFLT and ≥1 sector in TMT were used to this end in (**b**).

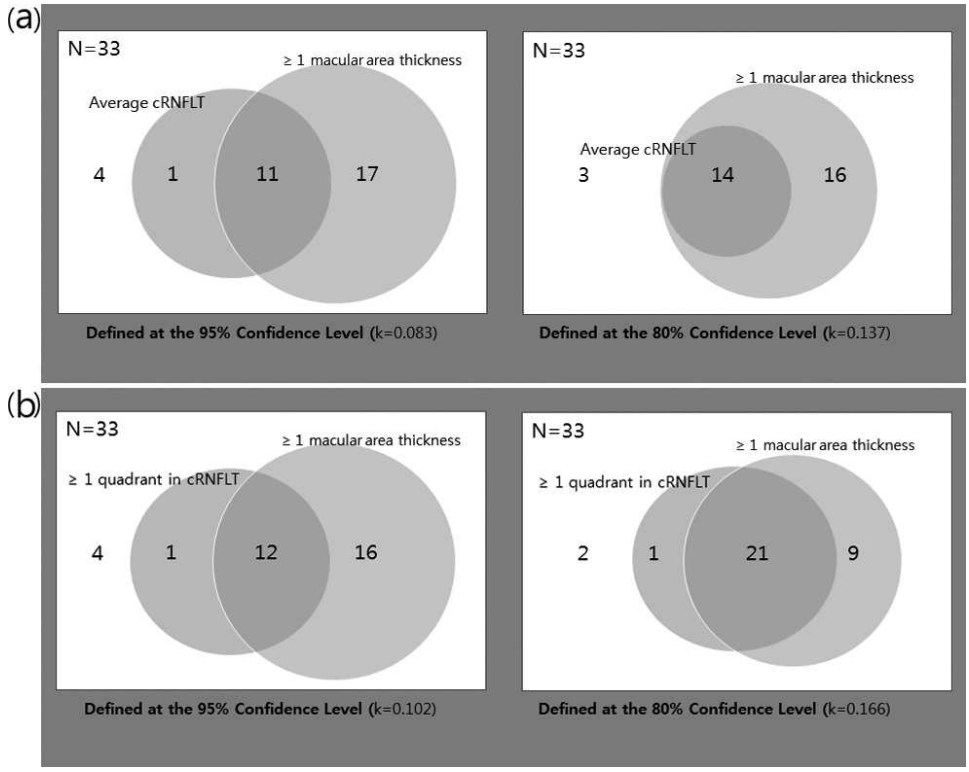

Figure 3. An area-proportional Venn diagram showing agreement in terms of glaucoma progression detection at central 10° region when average cRNFLT and ≥1 sector in TMT were used to this end in (**a**) and when ≥1 quadrant in cRNFLT and ≥1 sector in TMT were used to this end in (**b**).

of reproducibility. When reproducibility is higher, as noted with TMT measurements compared with cRNFLT (average and quadrant) as indicated by COV, small changes in TMT can be detected with confidence.

Another explanation for the improved ability to detect progression with TMT measurement criterion compared with cRNFLT is that a large number of eyes with NTG were included in our series (around 90%) as these eyes constitute the predominant form of glaucoma in our part of the Asia. Previous studies have shown that eyes with NTG showed VF defects that were dense and more central than in patients with primary open-angle glaucoma.[47–49] This central area (within 10° from the fixation point) corresponds well with macular nerve fibers, as shown by the maps of Weber and colleagues[50] and Garway-Heath and colleagues.[51] Thus, the progression detection ability for structural change of TMT in the macula could theoretically be superior to cRNFLT in eyes with NTG as the damaged area in the macula continues to lose more nerve tissue with glaucoma progression.

In eyes with progressive VF progression occurring in the central 10° area, a diagnostic comparison between TMT and cRNFLT sector measurements showed that the TMT mode clearly offered significantly better progression detection abilities at both confidence level ($P < 0.001$ and 0.021, respectively, Table 6). The most likely explanation is that RNFL damage in NTG eyes usually occurs closer to the center of the fovea, with associated VF defects and thereafter spreads to the surrounding areas.[47,52] With early disease progression as in our patient series, macular change noted in TMT measurements may be the first to be detected, followed by cRNFLT progression, which is remote from the fixation point in the periphery with further disease progression.

The specificity for criterion based on average cRNFLT was 85.0% using criteria corresponding to the upper 95% limit of test–retest variability defined at the 95% confidence level. The explanation for this lower specificity includes a different testing environment, patient characteristics, and image quality in spite of meeting required signal strength for the inclusion criteria between the two stable groups. Despite excellent COV associated with TMT measurements from a stable control group, the specificities based on TMT measurement were 77.5% and 62.5%, respectively (Table 5). The explanation for this lower specificity associated with TMT criterion is that the specificity was tested on a different glaucoma group, which can result in variability of data due to a different testing environment, patient cooperation, and image quality despite having a stable VF.

Agreement of progression detection between TMT and cRNFLT was poor for both average and sector data. This finding may indicate that there may be temporal and spatial differences in glaucoma progression between the two anatomical sites. To support this hypothesis, TMT measurement was found to be more sensitive in the detection of VF progression close to the fixation point than cRNFLT measurement. Previous studies have also demonstrated that poor agreement between structures using confocal scanning laser ophthalmoscopy (cSLO) and HFA progression was observed at various stages of the disease.[40,42,53,54] Strouthidis et al. have shown that in subjects with ocular hypertension, 21.2% progressed by cSLO criteria alone and 20.2% by SAP alone, and 12.1% progressed by both cSLO and SAP when examined prospectively over 7 years.[42] These cross-sectional studies suggest that some eyes progress in VF before they progress in the imaging devices, and there may be a disconnection between structure and function. It is also important to emphasize that with current technology, the strength of correlation between structure and function can vary according to patient factors, length of follow-up time and disease severity, or variability of measurements and instruments used.[54] Therefore, the longer we follow our patients, the better the agreement we obtain.

It is important to assess the strength of topographic match between the corresponding SD-OCT parameters and VF loss to confirm the utility of this device in detecting eyes with VF progression. In our study, the topographic match between structural and functional loss was strong as indicated by high percentages of topographic match using both TMT and cRNFLT parameters. This information may provide additional evidence that imaging devices such as SD-OCT can be used as surrogate markers to define endpoints in glaucoma clinical trials.

The results of our study must be interpreted with caution due to several limitations, including the relatively small sample size. Since it is difficult and time-consuming to recruit a sufficiently large database on progressive patients, it would be helpful if manufacturers of SD-OCT devices provide not only cross-sectional normative databases for glaucoma diagnosis, but also a reference database for even-based analysis of progression that would include glaucoma patients with a wide range of damage tested within relatively short periods of time to define the statistical limits of test–retest variability. Another limitation is that only good quality scans with signal strengths greater than 6 were included in the analyses, which might have influenced the upper limit of the variability of our measurements. Caution should be taken when diagnosing glaucoma progression based on a series of test including both good and poor quality scans. In the current study, test–retest variability and associated sensitivity and specificity were obtained from patients with early glaucomatous VF loss. Since the test–retest variability is not necessarily the same in early stage glaucoma as it is in more advanced glaucoma, it is possible that the test–retest variability from early stage glaucoma may not be applicable to eyes with more advanced glaucoma. Finally, our topographic match between VF data and TMT map was based on a less-than-ideal relationship due to an inherent lack of consideration for nerve fiber distribution with ETDRS subfields. This might have inflated the strength of structure-function match between two parameters. Further refinement of the macular thickness map respecting the RNFL travel pattern will enhance the capability of glaucoma detection and progression with topographic match with VF function.

In summary, intersession measurement of cRNFLT and TMT parameters obtained with SD-OCT (Carl Zeiss Meditec Inc.) was found to have excellent reproducibility, providing evidence that these parameters have a potential to be used in the longitudinal assessment of glaucoma progression. Based on event-based analysis using our reproducibility data, TMT measurement outperformed cRNFLT parameters for detecting glaucoma progression. In our subgroup analysis, the diagnostic performance of the TMT data in terms of detecting disease progression improved in those eyes in which VF defects were close to the fixation point.

References

1. Quigley HA, Dunkelberger GR, Green WR. Retinal ganglion cell atrophy correlated with automated perimetry in human eyes with glaucoma. *Am J Ophthalmol*. 1989;107:453–464.
2. Kanadani FN, Hood DC, Grippo TM, et al. Structural and functional assessment of the macular region in patients with glaucoma. *Br J Ophthalmol*. 2006;90:1393–1397.
3. Leung CK, Chan WM, Yung WH, et al. Comparison of macular and peripapillary measurements for the detection of glaucoma: an optical coherence tomography study. *Ophthalmology*. 2005;112:391–400.
4. Wollstein G, Ishikawa H, Wang J, Beaton SA, Schuman JS. Comparison of three optical coherence tomography scanning areas for detection of glaucomatous damage. *Am J Ophthalmol*. 2005;139:39–43.
5. Desatnik H, Quigley HA, Glovinsky Y. Study of central retinal ganglion cell loss in experimental glaucoma in monkey eyes. *J Glaucoma*. 1996;5:46–53.
6. Zeimer R, Asrani S, Zou S, Quigley H, Jampel H. Quantitative detection of glaucomatous damage at the posterior pole by retinal thickness mapping. A pilot study. *Ophthalmology*. 1998;105:224–231.
7. Seong M, Sung KR, Choi EH, et al. Macular and peripapillary retinal nerve fiber layer measurements by spectral domain optical coherence tomography in normal-tension glaucoma. *Invest Ophthalmol Vis Sci*. 2010;51:1446–1452.
8. Chang RT, Knight OJ, Feuer WJ, Budenz DL. Sensitivity and specificity of time-domain versus spectral-domain optical coherence tomography in diagnosing early to moderate glaucoma. *Ophthalmology*. 2009;116:2294–2299.
9. Moreno-Montanes J, Anton A, Olmo N, et al. Misalignments in the retinal nerve fiber layer evaluation using cirrus high-definition optical coherence tomography. *J Glaucoma*. 2011; 20:559–565.
10. Leung CK, Ye C, Weinreb RN, et al. Retinal nerve fiber layer imaging with spectral-domain optical coherence tomography a study on diagnostic agreement with Heidelberg Retinal Tomograph. *Ophthalmology*. 2010;117:267–274.
11. Jeoung JW, Park KH. Comparison of Cirrus OCT and Stratus OCT on the ability to detect localized retinal nerve fiber layer defects in preperimetric glaucoma. *Invest Ophthalmol Vis Sci*. 2010;51:938–945.
12. Kang SY, Sung KR, Na JH, et al. Comparison between deviation map algorithm and peripapillary retinal nerve fiber layer measurements using Cirrus HD-OCT in the detection of localized glaucomatous visual field defects. *J Glaucoma*. 2012;21:372–378.
13. Lee S, Sung KR, Cho JW, Cheon MH, Kang SY, Kook MS. Spectral-domain optical coherence tomography and scanning laser polarimetry in glaucoma diagnosis. *Jpn J Ophthalmol*. 2010;54:544–549.
14. Sung KR, Kim JS, Wollstein G, Folio L, Kook MS, Schuman JS. Imaging of the retinal nerve fibre layer with spectral domain optical coherence tomography for glaucoma diagnosis. *Br J Ophthalmol*. 2011;95:909–914.
15. Park SB, Sung KR, Kang SY, Kim KR, Kook MS. Comparison of glaucoma diagnostic capabilities of Cirrus HD and Stratus optical coherence tomography. *Arch Ophthalmol*. 2009;127: 1603–1609.
16. Mwanza JC, Chang RT, Budenz DL, et al. Reproducibility of peripapillary retinal nerve fiber layer thickness and optic nerve head parameters measured with cirrus HD-OCT in glaucomatous eyes. *Invest Ophthalmol Vis Sci*. 2010;51:5724–5730.
17. Garas A, Toth M, Vargha P, Hollo G. Comparison of repeatability of retinal nerve fiber layer thickness measurement made using the RTVue Fourier-domain optical coherence tomograph and the GDx scanning laser polarimeter with variable or enhanced corneal compensation. *J Glaucoma*. 2010;19:412–417.
18. Gonzalez-Garcia AO, Vizzeri G, Bowd C, Medeiros FA, Zangwill LM, Weinreb RN. Reproducibility of RTVue retinal nerve fiber layer thickness and optic disc measurements and agreement with Stratus optical coherence tomography measurements. *Am J Ophthalmol*. 2009;147:1067–1074.
19. Leung CK, Cheung CY, Weinreb RN, et al. Retinal nerve fiber layer imaging with spectral-domain optical coherence tomography: a variability and diagnostic performance study. *Ophthalmology*. 2009;116:1257–1263.
20. Menke MN, Dabov S, Knecht P, Sturm V. Reproducibility of retinal thickness measurements in healthy subjects using Spectralis optical coherence tomography. *Am J Ophthalmol*. 2009;147:467–472.

21. Sung KR, Cho JW, Lee S, et al. Characteristics of visual field progression in medically treated normal-tension glaucoma patients with unstable ocular perfusion pressure. *Invest Ophthalmol Vis Sci*. 2011;52:737–743.
22. Ferreras A, Pablo LE, Garway-Heath DF, Fogagnolo P, Garcia-Feijoo J. Mapping standard automated perimetry to the peripapillary retinal nerve fiber layer in glaucoma. *Invest Ophthalmol Vis Sci*. 2008;49:3018–3025.
23. Anderson DR. *Automated static perimetry*. St. Louis, MO: Mosby; 1992;91–137.
24. Landis JR, Koch GG. The measurement of observer agreement for categorical data. *Biometrics*. 1977;33:159–174.
25. Sung KR, Sun JH, Na JH, Lee JY, Lee Y. Progression detection capability of macular thickness in advanced glaucomatous eyes. *Ophthalmology*. 2012;119:308–313.
26. Vizzeri G, Weinreb RN, Gonzalez-Garcia AO, et al. Agreement between spectral-domain and time-domain OCT for measuring RNFL thickness. *Br J Ophthalmol*. 2009;93:775–781.
27. Kim JS, Ishikawa H, Sung KR, et al. Retinal nerve fibre layer thickness measurement reproducibility improved with spectral domain optical coherence tomography. *Br J Ophthalmol*. 2009;93:1057–1063.
28. Garas A, Vargha P, Hollo G. Reproducibility of retinal nerve fiber layer and macular thickness measurement with the RTVue-100 optical coherence tomograph. *Ophthalmology*. 2010;117:738–746.
29. Heijl A, Lindgren A, Lindgren G. Test-retest variability in glaucomatous visual fields. *Am J Ophthalmol*. 1989;108:130–135.
30. Boeglin RJ, Caprioli J, Zulauf M. Long-term fluctuation of the visual field in glaucoma. *Am J Ophthalmol*. 1992;113:396–400.
31. Chauhan BC, Johnson CA. Test-retest variability of frequency-doubling perimetry and conventional perimetry in glaucoma patients and normal subjects. *Invest Ophthalmol Vis Sci*. 1999;40:648–656.
32. Henson DB, Chaudry S, Artes PH, Faragher EB, Ansons A. Response variability in the visual field: comparison of optic neuritis, glaucoma, ocular hypertension, and normal eyes. *Invest Ophthalmol Vis Sci*. 2000;41:417–421.
33. Blumenthal EZ, Sample PA, Berry CC, et al. Evaluating several sources of variability for standard and SWAP visual fields in glaucoma patients, suspects, and normals. *Ophthalmology*. 2003;110:1895–1902.
34. Sihota R, Gulati V, Agarwal HC, Saxena R, Sharma A, Pandey RM. Variables affecting test-retest variability of Heidelberg Retina Tomograph II stereometric parameters. *J Glaucoma*. 2002;11:321–328.
35. Strouthidis NG, White ET, Owen VM, Ho TA, Hammond CJ, Garway-Heath DF. Factors affecting the test-retest variability of Heidelberg retina tomograph and Heidelberg retina tomograph II measurements. *Br J Ophthalmol*. 2005;89:1427–1432.
36. Zangwill L, Berry CA, Garden VS, Weinreb RN. Reproducibility of retardation measurements with the nerve fiber analyzer II. *J Glaucoma*. 1997;6:384–389.
37. Paunescu LA, Schuman JS, Price LL, et al. Reproducibility of nerve fiber thickness, macular thickness, and optic nerve head measurements using StratusOCT. *Invest Ophthalmol Vis Sci*. 2004;45:1716–1724.
38. DeLeon Ortega JE, Sakata LM, Kakati B, et al. Effect of glaucomatous damage on repeatability of confocal scanning laser ophthalmoscope, scanning laser polarimetry, and optical coherence tomography. *Invest Ophthalmol Vis Sci*. 2007;48:1156–1163.
39. Na JH, Sung KR, Baek S, et al. Detection of glaucoma progression by assessment of segmented macular thickness data obtained using spectral domain optical coherence tomography. *Invest Ophthalmol Vis Sci*. 2012;53:3817–3826.
40. Artes PH, Chauhan BC. Longitudinal changes in the visual field and optic disc in glaucoma. *Prog Retin Eye Res*. 2005;24:333–354.
41. Wollstein G, Schuman JS, Price LL, et al. Optical coherence tomography longitudinal evaluation of retinal nerve fiber layer thickness in glaucoma. *Arch Ophthalmol*. 2005;123:464–470.
42. Strouthidis NG, Scott A, Peter NM, Garway-Heath DF. Optic disc and visual field progression in ocular hypertensive subjects: detection rates, specificity, and agreement. *Invest Ophthalmol Vis Sci*. 2006;47:2904–2910.
43. Leung CK, Cheung CY, Weinreb RN, et al. Evaluation of retinal nerve fiber layer progression in glaucoma: a study on optical coherence tomography guided progression analysis. *Invest Ophthalmol Vis Sci*. 2010;51:217–222.
44. Leung CK, Liu S, Weinreb RN, et al. Evaluation of retinal nerve fiber layer progression in glaucoma a prospective analysis with neuroretinal rim and visual field progression. *Ophthalmology*. 2011;118:1551–1557.
45. Vizzeri G, Bowd C, Weinreb RN, et al. Determinants of agreement between the confocal scanning laser tomograph and standardized assessment of glaucomatous progression. *Ophthalmology*. 2010;117:1953–1959.
46. Alencar LM, Zangwill LM, Weinreb RN, et al. Agreement for detecting glaucoma progression with the GDx guided progression analysis, automated perimetry, and optic disc photography. *Ophthalmology*. 2010;117:462–470.
47. Caprioli J, Spaeth GL. Comparison of visual field defects in the low-tension glaucomas with those in the high-tension glaucomas. *Am J Ophthalmol*. 1984;97:730–737.
48. Koseki N, Araie M, Suzuki Y, Yamagami J. Visual field damage proximal to fixation in normal- and high-tension glaucoma eyes. *Jpn J Ophthalmol*. 1995;39:274–283.
49. Araie M, Yamagami J, Suziki Y. Visual field defects in normal-tension and high-tension glaucoma. *Ophthalmology*. 1993;100:1808–1814.
50. Weber J, Dannheim F, Dannheim D. The topographical relationship between optic disc and visual field in glaucoma. *Acta Ophthalmol*. 1990;68:568–574.
51. Garway-Heath DF, Poinoosawmy D, Fitzke FW, Hitchings RA. Mapping the visual field to the optic disc in normal tension glaucoma eyes. *Ophthalmology*. 2000;107:1809–1815.
52. Kook MS, Lee SU, Sung KR, et al. Pattern of retinal nerve fiber layer damage in Korean eyes with normal-tension glaucoma and hemifield visual field defect. *Graefes Arch Clin Exp Ophthalmol*. 2002;240:448–456.
53. Hood DC, Anderson SC, Wall M, Kardon RH. Structure versus function in glaucoma: an application of a linear model. *Invest Ophthalmol Vis Sci*. 2007;48:3662–3668.
54. Lamparter J, Russell RA, Schulze A, Schuff AC, Pfeiffer N, Hoffmann EM. Structure-function relationship between FDF, FDT, SAP, and scanning laser ophthalmoscopy in glaucoma patients. *Invest Ophthalmol Vis Sci*. 2012;53:7553–7559.